Published in final edited form as:
Mol Cancer Ther. 2011 December ; 10(12): 2330–2339. doi:10.1158/1535-7163.MCT-11-0202.

Differential expression of uridine phosphorylase in tumors contributes to an improved fluoropyrimidine therapeutic activity

Deliang Cao[†], **Amy Ziemba**[¥], **James McCabe**[‡], **Ruilan Yan**[†], **Laxiang Wan**[Ψ], **Bradford Kim**[Ψ], **Michael Gach**[¥], **Stuart Flynn**[‡], and **Giuseppe Pizzorno**[Ψ,¥]

[†]Department of Medical Microbiology, Immunology, and Cell Biology, Simmons/Cooper Cancer Institute, Southern Illinois University School of Medicine. 911 North Rutledge Street, Springfield, IL 62702

[Ψ]Department of Internal Medicine (Medical Oncology), Yale University School of Medicine. 333 Cedar Street, New Haven, CT 06520

[‡]Department of Pathology, Yale University School of Medicine. 333 Cedar Street, New Haven, CT 06520

[¥]Division of Drug Development, Nevada Cancer Institute, One Breakthrough Way, Las Vegas, NV 89117

Abstract

Abrogation of uridine phosphorylase (UPase) leads to abnormalities in pyrimidine metabolism and host protection against 5-fluorouracil (5-FU) toxicity. We elucidated the effects on the metabolism and antitumor efficacy of 5-FU and Capecitabine in our *UPase* knockout (*UPase* −/−) model.

Treatment with 5-FU (85 mg/kg) or Capecitabine (1000 mg/kg) 5 days a week for 4 weeks caused severe toxicity and structural damage to the intestines of wild-type (WT) mice, but not in *UPase* −/− animals. Capecitabine treatment resulted in a 70% decrease in blood cell counts of WT animals, with only a marginal effect in *UPase* −/− mice. UPase expressing colon 38 tumors implanted in *UPase* −/− mice revealed an improved therapeutic efficacy when treated with 5-FU and Capecitabine due to the higher maximum tolerated dose for fluoropyrimidines achievable in UPase −/− mice.

^{19}F-MRS evaluation of Capecitabine metabolism in tumors revealed similar activation of the pro-drug in *UPase* −/− mice compared to WT. In WT mice, approximately 60% of Capecitabine was transformed over 3 hours into its active metabolites, while 80% was transformed in tumors implanted in *UPase* −/− mice. In *UPase* −/− mice, prolonged retention of 5′dFUR allowed a proportional increase in tumor tissue. The similar presence of fluorinated catabolic species confirms that dihydropyrimidine dehydrogenase activity was not altered in *UPase* −/− mice.

Overall, these results indicate the importance of UPase in the activation of fluoropyrimidines, the effect of uridine in protecting normal tissues, and the role for tumor-specific modulation of the phosphorolytic activity in 5-FU or Capecitabine-based chemotherapy.

Keywords

Uridine phosphorylase; gene knockout; fluoropyrimidines; bone marrow; gastrointestinal tract

Correspondence should be addressed to: Giuseppe Pizzorno, Ph.D., Pharm.D., Division of Drug Development, Nevada Cancer Institute, One Breakthrough Way, Las Vegas, NV 89135. Tel. (702) 822-5380, Fax: (702) 944-2369, gpizzorno@nvcancer.org.

Introduction

Uridine phosphorylase (UPase), a phosphorolytic enzyme ubiquitously expressed, has been shown to be induced in various human solid tumors compared to surrounding normal tissues (1–2). This is possibly due to frequent mutations of *p53* (a suppressor of *UPase* gene expression) (3) or higher expression of various cytokines (inducers of *UPase* expression) in tumor tissues (4–5). Because of its increased expression in tumors, it is important to determine the role of UPase in the activation and antitumor activity of fluoropyrimidines, such as 5-fluorouracil (5-FU), 5′-deoxy-5-fluorouridine (5′DFUR), and Capecitabine. *UPase* knockout (*UPase* −/−) mice provide an ideal model for this study (6).

The antitumor activity of 5-FU stems from its proximal metabolites, 5-fluoro-2′-deoxyuridine-5′-monophosphate (FdUMP), 5-fluorouridine-5′-triphosphate (FUTP), and 5-fluoro-2′-deoxyuridine-5′-triphosphate (FdUTP). These active metabolites either inhibit the activity of thymidylate synthase (TS) or incorporate into RNA or DNA, leading to nucleic acid dysfunction and cell death (7–8). Several studies have indicated the role of UPase in fluoropyrimidine activation, including the anabolism of 5-FU into 5-fluorouridine with subsequent phosphorylation to 5-fluorouridine-monophosphate (FUMP) and the phosphorolysis of the prodrug 5′DFUR into 5-FU (9–11). Using human and murine cancer cell lines, Peters, *et al.* (12) reported that 5-fluorouridine (FUrd) synthesis was directly correlated to the intracellular UPase activity. In colon 26 tumor cells, a mixture of tumor necrosis factor-α (TNF-α), interleukin-1α (IL-1α), and interferon-γ (IFN-γ) efficiently enhanced 5-FU cytotoxicity 2.7-fold and 5′DFUR cytotoxicity 12.4-fold, due to induction of UPase activity (5). However, in most experimental models the contribution of UPase to fluoropyrimidine activity has been controversial due to the co-existence of other related metabolic enzymes, thymidine phosphorylase (TPase) and orotate phosphoribosyl transferase (OPRTase). OPRTase participates in the *de novo* pyrimidine synthesis pathway, directly converting 5-FU to FUMP in the presence of 5-phosphoribosyl-1-pyrophosphate (PRPP) (13), while TPase contributes to the formation of fluorodeoxyuridine (dFUrd) (14). In addition, TPase is also involved in the phosphorolysis of 5′DFUR into 5-FU (15). We have investigated the effect of UPase on the antiproliferative activity of fluoropyrimidines using a gene-targeted cell model, *UPase* gene-knockout murine embryonic stem (ES) cells, and found that the abrogation of UPase in these cells resulted in an 8-and 16-fold increase in the IC50's of 5-FU and 5′DFUR, respectively (9). The unique genetic modification of UPase activity directly confirmed the role of UPase in fluoropyrimidine metabolism and activation. However, this *in vitro* system does not allow the investigation of the metabolic kinetics and tissue distributions of fluoropyrimidines. In addition, the cultured cells are also limited for the study of Capecitabine, a prodrug of 5-FU, because its activation is precluded by the lack of carboxylesterase (16). In this report we investigated the metabolic kinetics and tissue distributions of 5-FU in *UPase* −/− mice, and evaluated the histological basis of host toxicity of Capecitabine.

A major drawback of fluoropyrimidine-based chemotherapy are the severe dose-limiting side effects at the level of the bone marrow and gastrointestinal tract, often resulting in therapeutic failure (17–18). Therefore, the development of prodrugs or modulatory strategies to increase tumor selectivity is an important effort to improve the therapeutic efficacy of fluoropyrimidines. Using *UPase* −/− mouse-based colon tumor models, we assessed the effect of the tumor-specific modulation of UPase activity on tumor selectivity and antitumor efficacy of 5- FU and Capecitabine. The results provide important information for clinical approaches to improve the therapeutic outcomes of fluoropyrimidine-based regimens.

Materials and Methods

Animals and Cell Lines

Wild-type and *UPase* −/− mice were produced and maintained as previously described (6). All experiments were performed according to Yale University and NVCI guidelines for the humane treatment of animals. Colon 38 murine adenocarcinoma cells (MC38) were originally obtained from the Southern Research Institute, Birmingham, AL (19) and authenticated by flow-cytometry before implantation.

In vivo toxicity of Capecitabine

Toxicity of Capecitabine was evaluated in wild-type and *UPase* −/− mice at 8–12 weeks. Mice were randomly grouped according to gender and body weight, six mice per group. Capecitabine (Xeloda) was suspended in 40 mmol/L citrate buffer (pH 6.0)/5% wt/vol of hydroxypropylmethylcellulose and administered by oral gavage at 1,000 to 1,375 mg/kg daily, 5 days a week for 4 weeks. Animal weights were measured daily to monitor the toxicity. The dose leading to 15–20% weight loss was defined as the maximum tolerated dose (MTD). Observations of a given treatment group ceased when animals lost more than 20% of their body weight or after the first mouse death occurred in the group. All the experiments were conducted at least in duplicate.

Antitumor activity of 5-FU and Capecitabine

To observe the therapeutic efficacy of fluoropyrimidine treatment, murine colon 38 tumor suspension (200 μl) was implanted into both flanks of the mice (19). Colon 38 expresses wild-type UPase and its enzymatic activity was found to be similar once transplanted in wild-type or *UPase* −/− mice (Table 1). When the tumors grew to an average size of 100–150 mg, animals were randomly assigned into groups, six mice in each group with comparable average body weight and tumor size. Tumor size was determined by measuring the two axes of the tumor (L, longest axis, and W, shortest axis) with a vernier caliper, and weight estimated according to the following formula: Tumor-weight (mg) = $W^2 \times L/2$ (19). 5-FU was administered weekly by intraperitoneal injection at 85 and 150 mg/kg, and Capecitabine was administered orally on a daily basis at 1,000 and 1,375 mg/kg, 5 days a week.

Metabolism and tissue distribution of 5-FU

[6-^{3}H]-5-FU (20Ci/mmol) was intravenously administered to mice (200 mg/kg) through the tail vein. At the indicated time points, animals were anesthetized and blood collected by retroorbital bleeding. Plasma was separated by centrifugation at 2,000 × *g*, 4°C for 5 min, extracted with 2 volumes of 15% trichloroacetic acid (TCA) at 14,000 rpm for 10 min, and neutralized with an equal volume of trioctylamine-freon (45:55, v:v). Aqueous phase was used for HPLC analysis (19). Tissues frozen in liquid nitrogen were weighed and homogenized in 2 volumes of 15% TCA and the supernatant extracted for HPLC analysis as described for plasma. [^{3}H]-5-fluorouridine and [^{3}H]-5-fluorouracil were separated on a C18 reverse-phase Microsorb column (250×4.6 mm, Varian) using mobile phase ddH_2O:10mM H_3PO_4:30μM heptane sulfonic acid (94:5:1, pH 3.1) at 1.0 ml/min by cooling the column at 8°C. 5-Fluororibonucleotides (FUXP), measured as FUMP obtained after boiling the samples at 100°C for 10 min, were separated using a Whatman Partisil-10-SAX anion-exchange column with 5 mM sodium phosphate mobile phase (pH 3.3) at 1.4 ml/min. Elution was fractioned and radioactivity determined using a scintillation counter (Beckman). For RNA incorporation of 5-FU, liver, tumor and intestinal tissues were weighed and total RNA extracted using Trizol reagent (Invitrogen) (9). DNA was isolated by suspending the precipitated nucleic acidsin lysis buffer, then incubating the suspension at 55°C overnight

and subsequently for 1 hat 37°C with RNase A/T1. To precipitate DNA, an equal volume of 2-propanol was added and mixed until precipitation was complete and further by extractions with phenol/chloroform/iso-amylalcohol (50/49/1 v/v/v) and chloroform/iso-amylalcohol (49/1 v/v). DNA was precipitated with an equal volume of 2-propanol and reconstituted in 0.5 ml digestion buffer at 55°C. For measurement of concentration and purity, optical density was measured at 260 and 280 nm. The radioactivity in DNA/RNA was determined by scintillation counter (20).

Analysis of FdUMP Concentration in Tumors

Colon 38 tumors were excised 4 hours after administration of 200 mg/kg of 5-FU and immediately frozen in liquid nitrogen. Frozen tumors were pulverized, suspended in three volumes of Tris-HCl buffer (pH 7.4) and extracted with TCA (final concentration 5%). The supernatant was neutralized and stored until analysis for FdUMP. FdUMP was measured using a dilution assay based on the capacity of FdUMP present in tumors to inhibit the binding of [6-^{3}H]-FdUMP to Lactobacillus casei thymidylate synthase (21).

Enzyme activity assays

UPase activity was measured by conversion of uridine to uracil as described previously (9). TPase activity was determined by measuring the conversion of thymidine into thymine using [^{3}H]-thymidine as substrate and 100 μM 5-Benzylacyclouridine (BAU, a specific UPase inhibitor). OPRTase activity was assayed by measuring the formation of 5-Fluorouridine monophosphate from 5-Fluorouracil in the presence of PRPP (9). A 100 μl reaction mixture containing 200 μM [^{14}C]-5-fluorouracil, 1 mM PRPP, 100 μM $MgCl_2$, 50 mM Tris-Cl (pH 7.6) and 100 μM BAU was incubated at 37°C for one hour. UK was detected by measuring the conversion of uridine into UMP in the presence of ATP (6). The reaction was performed in a 100 μl volume with 200 μM [^{14}C]-uridine, 1 mM ATP, 100 μM $MgCl_2$, 50 mM Tris-Cl (pH 7.6) and 100 μM BAU. The resultant [^{14}C]-UMP was separated on TLC plates and determined by scintillation counting. DPD activity was measured by determining the conversion of uracil into dihydrouracil. The assay mixture contained 200 mM NADPH and 8.25 mM [^{14}C]-uracil in a solution constituted by 35 mM potassium phosphate (pH 7.4), 2.5 mM magnesium chloride, 10 mM 2-mercaptoethanol. The formed [^{14}C]-dihydrouracil was separated on TLC plates and radioactivity determined (22).

MRS Evaluation of Capecitabine Metabolism

Wild-type or *UPase* −/− mice bearing Colon 38 tumors were treated orally with 1000 mg/kg Capecitabine. Animals were anesthetized with isoflurane (2–3% induction and 1–2% maintenance) along with 0.5 LPM O_2. MRI and MRS were performed using a Bruker 7T/20 Biospin MRI (Billerica, MA), equipped with a dual-tuned 7 cm ID ^{1}H/^{19}F volume coil (Bruker) and a 15 mm ID detunable receive-only ^{19}F surface coil (Doty Scientific). The surface coil was placed over the region of interest and the animal secured to minimize the effects of motion on the MR data. A ^{1}H T_2-weighted TurboRare sequence [repeat time (TR): 2330 ms, echo time (TE): 36 ms, Rare factor: 8, matrix: 256×256, field of view (FOV): 4 cm] was used for positioning and structural imaging of the animal and delineating the region of interest. A ^{1}H point-resolved spectroscopy sequence (PRESS) was used for magnetic field shimming over the ROI (TR: 721 ms, TE: 20 ms, flip angle: 90°) (23).

^{19}F spectra were acquired and averaged during 27.5 min blocks (3300 FIDs, TR: 0.5 s, spectral width: 60 kHz, points/FID: 890, flip angle: 60°, RF pulse duration: 50μs) for 3 hours. The ^{19}F MRS data were analyzed using Bruker's Topspin application. The rate of Capecitabine activation and buildup of the intermediate molecules were evaluated.

Peripheral blood cells counting

Peripheral blood samples were collected from mice treated with Capecitabine at 1000 mg/kg for 4 weeks. Number of erythrocytes per μl and hematocrit values were determined using a Coulter counter (Model ZF, Coulter Electronics). Hemoglobin was measured by a hemoglobinometer (Coulter Electronics) using the cyanmethemoglobin method. Numbers and subtypes of white blood cells were determined on 50 μl of peripheral blood, after red blood cells were osmotically lysed, using a flow cytometer (Becton Dickinson). Total and differential white blood cell counts were determined. To determine the platelet counts, the white blood cell preparations were diluted at 1:10 and the counts were obtained by appropriately adjusting gains and threshold (24).

Histological examination of small and large intestine

The intestinal tract, the small intestine and colon were excised from mice treated with 5-FU (85 mg/kg) or Capecitabine (1000 mg/kg) for 4 weeks. The isolated tissues were then fixed in formal fixative, and transverse sections (5 μm) were prepared for staining with hematoxylin and eosin. Histological changes of the tissues were evaluated under light microscopy.

Results

In a previous study, we reported that the abrogation of UPase in mice led to a decrease in 5-FU host toxicity (6). However, it was not clear whether this host protection resulted from a reduced activation of 5-FU through the pyrimidine salvage pathway or from the protection of increased uridine in the plasma and tissues, due to the elimination of UPase activity. In this study on the *UPase* −/− mouse model, we investigated metabolism and tissue distribution of 5-FU and examined the pathological basis of 5-FU and Capecitabine toxicity, and we evaluated the effect of UPase abrogation on the antitumor activity of 5-FU and Capecitabine.

Plasma clearance of 5-FU displayed a faster rate in *UPase* −/− mice than in wild-type with a T ½ of 26.3 minutes versus 37.9 minutes and clearance of 29.4 versus 18.1 ml/min/kg, respectively for *UPase* −/− and wild-type C57 BL6 mice (Table 2). This indicates that alterations in the anabolic pathway of 5-FU due to UPase abrogation significantly affected its clearance rate, consequently reducing exposure to the drug as indicated by a significantly smaller systemic exposure with an AUC of 84.5 mM-min in wild-type compared to 52.3 mM-min for the knockout mice. Normally, plasma 5-FU is mainly removed via the dihydropyrimidine dehydrogenase (DPD)-initiated degradation pathway (25). When the drug is administered orally or intraperitoneally, liver represents the major site of 5-FU metabolism with more than 85% of a given dose of the fluoropyrimidine eliminated through the rapid formation of dihydrofluorouracil (26). While the expression and the enzymatic activity of DPD in the liver of both mice are virtually similar (Table 1), the elevated 5-FU clearance in *UPase* −/− mice possibly suggests a reduced competition of uracil for DPD, in which uracil formation from uridine degradation is blocked because of the lack of UPase. However, the plasma pharmacokinetics of 5-fluorouridine (FUrd), following 5-FU delivery, displayed a significant difference in *UPase* −/− mice (Table 2). In wild-type mice, FUrd appeared in plasma within 5 min following i.p. administration of 5-FU (200 mg/kg), reaching nearly 4 μM at 10 min. Thereafter, FUrd concentration quickly declined to an undetectable level at 4 hours. Plasma FUrd in *UPase* −/− mice was barely detectable at 10 min and its peak appeared 1 hour after administration of the same dose of 5-FU. The clearance of plasma FUrd was significantly slower in *UPase* −/− mice than in wild-type, and a considerable amount of FUrd was still detected 4 hours after 5-FU administration resulting in a significantly higher AUC (316 vs. 105μM-min) (Table 2). In wild-type mice, UPase

rapidly catalyzed the formation of FUrd from administered 5-FU. However, in *UPase* −/− mice, plasma FUrd was possibly originated from the degradation of FUMP synthesized by OPRTase-catalyzed *de novo* pathway (13, 27), and eventually cleared by kidney excretion (6). As a result, a delay occurred in plasma peak concentration of FUrd, accompanied with a prolonged half-life in *UPase* −/− mice.

The liver is the major metabolic organ for 5-FU, and the gastrointestinal system represents one of the major toxicity targets for fluoropyrimidines. Therefore, the 5-FU metabolic pharmacokinetics and distribution in these tissues were examined. Overall, 5-FU and FUrd showed similar metabolic patterns in these tissues unlike that in plasma (Figure 1A and 1B). 5-FU was cleared slightly faster in both liver and intestines of *UPase* −/− mice, but with no statistical significance ($P>0.05$) compared to wild-type animals; while the formation and metabolism of FUrd varied with *UPase* expression status and tissue types. In wild-type intestinal tissues, a high level of FUrd was detected at 10 min after i.p. administration of 5-FU (200 mg/kg), but declined rapidly within 30 min and still maintained detectable levels after 4 hours. In *UPase* −/− intestinal tissues, however, FUrd appeared at 30 min and peaked at 60 min after 5-FU delivery. However, in *UPase* −/− liver tissues, FUrd was present at 10 min and reached a peak concentration at 30 minutes, 3-fold higher than that in the intestines, indicating an active 5-FU anabolism through pyrimidine *de novo* synthesis in liver. Similar to that in the intestines, the clearance of FUrd was much faster in wild-type liver than that in *UPase* −/− (Figure 1B). Taken together, these data indicate the important role of UPase in 5-FU/FUrd metabolism in normal intestinal and liver tissues, supporting our previous observation that ribose-1-phosphate is not a rate-limiting factor in the 5-FU anabolic metabolism catalyzed by UPase (9).

The incorporation of 5-FU into RNA is important for its antiproliferative activity (28) but has also been linked to the toxic effect of fluoropyrimidines (29–30). Therefore, we included in our investigation the measurement of 5-fluoro-ribonucleotide (FUXP) levels and 5-fluoro-RNA amounts in liver, gastrointestinal tract and transplanted Colon 38 tumor. As shown in Figure 1C and 1D, the levels of FUXP and 5-fluoro-RNA were significantly higher in wild-type liver and intestines than in *UPase* −/−. 5-FU incorporated into RNA of liver tissue started to be cleared within the first hour, while we observed a protracted accumulation in the RNA of the intestinal tissues of wild-type mice for more than 4 hours, providing the pharmacokinetic basis for the intestinal lesions caused by the fluoropyrimidines in the wild-type mice. The lower incorporation of 5-FU in the normal tissues of the *UPase* −/− mice, likely due to the competition of high uridine levels, confirms our previous observation of reduced in vivo host toxicity to 5-FU and a 75% higher MTD of 5-FU in this strain (6).

We observed significant differences in the concentration of uridine in plasma and normal tissues of wild-type mice compared to the *UPase* −/− (Table 3). Uridine concentration was elevated 3-fold in the intestine and kidney and up to 15-fold in spleen of *UPase*−/− mice compared to the corresponding wild-type tissues. In Colon 38 tumors transplanted in both wild-type and *UPase* −/− mice, we observed a reduced uridine concentration compared to the other tissues with levels similar to plasma concentrations. The elevation in tumor uridine concentration we determined in *UPase* −/− was highly significant ($p<0.01$) compared to the tumor in wild-type mice (7 vs. 1 μM), however the uridine concentration still remained almost 10-fold below the normal tissues concentrations (Table 3).

When we measured the incorporation of 5-FU in Colon 38 tumors, we observed 69.2+/−28.4 nmol/g into the RNA of tumors in wild-type mice and 64.6+/−26.9 nmol/g in tumors implanted in *UPase* −/− 4 hours after the administration of a 200 mg/kg dose of 5-FU. Also the incorporation of 5-FU into DNA was not significantly different between tumors grown in wild-type mice compared to *UPase* −/−, 367+/−57 fmol/μg of DNA and 431+/−83 fmol/

μg of DNA, respectively. The concentration of FdUMP present in Colon 38 tumors following a 200 mg/kg administration of 5-FU did not show any significant difference between the tumors implanted in the two different strains, 66+/−21 pmol/g of tissue of FdUMP in wild-type versus 72+/−13 in UPase −/− mice.

The role of UPase in the activation of 5′DFUR to 5-FU has also been determined in this study. Capecitabine (N^4-pentyloxycarbonyl-5′-deoxy-5-fluorocytidine) is a pro-drug of 5-FU, approved for the treatment of advanced breast and colon cancers (31–32). The carbamate modification facilitates its passage through the gastrointestinal mucosa without activation, leading to almost 100% oral bioavailability (33). In liver, Capecitabine is hydrolyzed by carboxylesterase to 5′-deoxy-5-fluorocytidine (5′DFCR) then converted to 5′DFUR by cytidine deaminase. 5′DFUR has no inherent cytotoxic activity, to exert its antiproliferative activity it must be hydrolyzed to 5-FU by UPase and TPase (17, 33). In this study, we assessed the effect of UPase on the host toxicity of Capecitabine using *UPase* −/− mice. A daily1000 mg/kg oral dose of Capecitabine caused nearly 20% weight loss in wild-type mice within 4 weeks; and 1,375 mg/kg led to the first death immediately preceding the third dose due to gastrointestinal bleeding (data not shown). In *UPase* −/− mice, however, no significant host toxicity was observed at doses up to 1,250 mg/kg and the higher dose of 1,375 mg/kg caused weight loss (15%) only comparable to that in wild-type mice at 1,000 mg/kg, further clarifying the role of UPase in the activation of 5′DFUR/Capecitabine. Possibly due to the significant TPase activity reported in mouse liver (6), which also contributes to conversion of 5′DFUR into 5-FU (15, 34), a larger MTD dose was not achieved in the *UPase* −/− mice.

As previously indicated, bone marrow and the gastrointestinal tract are the two major targets of fluoropyrimidines lesions (17–18). To understand the histological basis of this host protection by UPase abrogation, we further examined the pathological changes in the intestines and bone marrow of animals treated with 5-FU and Capecitabine. Peripheral blood cell counts were used to evaluate the hematological toxicity and intestinal transverse sections were examined following hematoxylin and eosin staining to evaluate the intestinal lesions. The treatment with Capecitabine (1,000 mg/kg) for 4 weeks caused a decrease of up to 70% in peripheral blood cells of wild-type animals. The alterations occurred in the hematocrit level (-40%), red blood cells (-44%), white blood cells (-72%) and subtypes, and platelets (-66%), indicating an overall effect on the regeneration and differentiation of bone marrow cells. These decreases in cell counts were minimal and not significant in the peripheral blood of *UPase* −/−mice, indicating that the abrogation of UPase activity and the high concentration of circulating uridine protected the bone marrow from Capecitabine-induced toxicity. A similar result was also observed in mice treated with 5-FU (data not shown).

The UPase abrogation also protected murine intestine from Capecitabine lesions. We observed a complete destruction of the villous architecture, crypts, and muscle layer in the intestines of wild-type mice treated with 1,000 mg/kg of Capecitabine for 4 weeks, but not in the intestines of *UPase* −/− mice exposed to the same treatments. This protection by UPase abrogation confirms the critical role of UPase in 5′DFUR/Capecitabine activation and toxicity.

To evaluate the clinical significance of host protection provided by UPase abrogation, we further assessed the antitumor efficacy of 5-FU and Capecitabine (Figure 2A). Treatments were initiated when the implanted tumors grew to an average size of 100 to 150 mg. 5-FU was used at 85 mg/kg (the MTD for wild-type mice) and 150 mg/kg (a dose shown to be tolerated only by *UPase* −/− mice) (7); and Capecitabine was administered at 1,000 mg/kg (the MTD for wild-type mice) and 1,375 mg/kg (a dose shown to be tolerated only by *UPase*

−/− mice). As presented in Figure 2B, a higher dose of 150 mg/kg of 5-FU efficiently controlled and reduced tumor size, while the standard 85 mg/kg dose of 5-FU only partially slowed down tumor growth in both strains. In the Capecitabine treatments, a 30% dose increase from 1,000 mg/kg to 1,300 mg/kg resulted in dramatic tumor growth inhibition in *UPase* −/− mice (Figure 2C), with complete disappearance of tumors in 10 of 11 mice. These data indicate that the tumor-specific modulation of UPase activity can greatly improve the antitumor efficacy of 5-FU and Capecitabine by allowing dose escalation without causing significant host toxicity.

To better evaluate the activation of Capecitabine and the potential differences in metabolism between Colon 38 tumors implanted in wild-type mice and in *UPase* −/− mice, we conducted a series of in vivo ^{19}F-MRS experiments using a 1,000 mg/kg oral dose of Capecitabine administered as a bolus. The in vivo spectra (Figure 3A) resolve five main fluorinated species, with the administered drug Capecitabine at 7 ppm upfield from the 5-FU signal, 5′-deoxy-5-fluorocytidine at 5 ppm, 5′-deoxy-5-fluorouridine at 3.5 ppm and the two main fluorinated metabolites, fluoroureidepropionic acid and α-fluoro-β-alanine, at −17 and −19 ppm respectively. As reported in Figure 3A, we detected all five fluorinated species mentioned starting 30 min after the oral administration of Capecitabine and were able to follow their presence over 3 hours of spectra acquisition. We observed in tumors implanted in wild-type mice that Capecitabine represented approximately 35% of the total fluorine signal, 5′dFCR corresponded to a similar percentage while 5′dFUR ranged from 25 to 30% of total fluorine. The two catabolites, FUPA and FβAL were approximately 5% of the total (Figure 3B). The tumors implanted in the *UPase* −/− mice showed that Capecitabine was approximately 15% of the total fluorine signal, 5′dFCR 45%, 5′dFUR 35% and the sum of the two catabolites ranged from 4 to 7% of the total (Figure 3C).

We were unable to capture the 5-FU signal consistently, likely due to the rapid transformation of 5-FU into 5-FUrd and its fluoronucleotides in colon 38 tumors expressing wild-type UPase. 5-FUrd and FUXP with their signals at 3.6 and 5.1 ppm, respectively, were impossible to quantitate given the overwhelming presence of 5′dFCR and 5′dFUR in the 3.5–5 ppm region.

Our data indicates that the genetically induced changes and the elevation in circulating uridine did not interfere with the carboxylesterases and cytidine deaminase in the activation of Capecitabine. Also, the comparable presence of 5-FU catabolites FUPA and FβAL in liver from wild-type and *UPase* −/− mice confirms the similar DPD enzymatic activity (Table 1) and qRT-PCR data (wt 1.0±0.1 versus 0.8±0.2 in *UPase* −/−) and therefore a similar rate of catabolic degradation for 5-FU in the two murine strains.

Discussion

UPase activity and expression has been shown to be elevated in many tumors including colorectal carcinomas, breast cancer, melanomas and lung adenocarcinomas (11). Several mechanisms have been uncovered, all leading to an increased expression in human tumors. We have previously reported that the expression of UPase is induced by TNF-α through the NF-κB pathway (11). Other groups have shown that EWS/ETS fusion proteins, playing a dominant oncogenic role in cell transformation in Ewings family tumors, induce UPase gene expression through interaction with the UPase promoter (35). More recently, PGC-1α/ERR-dependent up- regulation of UPase was shown to contribute to an increased enzymatic activity in colon and breast cancer cells (36). These results demonstrate that the elevation of UPase in tumor is a key contributor to the tumor-selectivity of 5-FU and Capecitabine. Unlike TPase, UPase is not associated with any identified angiogenic activity because of its limited catalytic activity on deoxy-nucleosides. It has been shown that 2-deoxyribose-1-

phosphate released from the deoxy-nucleoside by TPase activity can act as an endothelial-cell chemoattractant and angiogenic factor (37). This feature allows for a convenient modulation of the phosphorolytic activity in tumors by *UPase* gene transfer or delivery of specific inducers of *UPase* gene expression, such as cytokines. This modulation would not be complicated by possible tumor growth stimulation due to simultaneously induced angiogenesis, as is the case with TPase (38).

The data here presented establish once more the role of uridine in protecting normal tissues from the toxicity of fluoropyrimidines. In the normal tissues of *UPase*−/− mice we observed a constitutive uridine concentration above 50 μM, with the gut, the major target of 5- FU toxicity, at 90 μM. These concentrations have been found previously to be sufficient to provide adequate protection against 5-FU based chemotherapy regimens (39–40). Similarly, the concentration of uridine in Colon 38 tumors implanted in *UPase* −/− mice approximated the plasma uridine concentration of 7 μM indicating that the inability of some tumors to accumulate this nucleoside is likely due to the loss of the concentrative transport mechanism (41).

Several studies have demonstrated the capacity of large doses of uridine to reduce 5-FU toxicity, without affecting its antitumor activity, if properly sequenced (42). Unfortunately, the administration of large doses of uridine, because of its rapid half-life, results in moderate to severe toxicity. Our laboratory has shown that this problem could be overcome by utilizing inhibitors of UPase, such as BAU, to conserve endogenous uridine with consequent elevation of its concentration in plasma and tissues. A phase I clinical trial of oral BAU administered as a single agent has shown the ability of this inhibitor to elevate the plasma uridine concentration 2–3 fold without significant host toxicity (43).

The combination ‘rescue regimens’ of 5-FU plus uridine were initially proposed to evaluate the hypothesis that the antitumor effect of 5-FU is primarily due to the inhibition of thymidylate synthase and the host toxicity mostly caused by the incorporation of the fluoropyrimidine into RNA (44). In vivo studies in a murine model and in vitro data (45-46) have clearly indicated that the incorporation of 5-FU into RNA appears to be the major cause of gastrointestinal toxicity, that uridine inhibited the incorporation and avoided the cytotoxic effect, whereas thymidine did not prevent 5-FU toxicity.

Clinical studies of 5-FU in combination with methotrexate and PALA have shown that patients tolerated combination therapy with delayed uridine up to a weekly dose of 750 mg/m^2 of 5-FU, with 25% experiencing moderate mucositis (grade II). In previous clinical trials without uridine, 4 out of 6 patients could not tolerate a 600 mg/m^2 dose of 5-FU because of mucositis, diarrhea and a decrease in performance status. Another study of high dose 5-FU with doxorubicin, high dose methotrexate and leucovorin, oral uridine administration allowed for dose intensification of 5-FU and ensured rescue from 5-FU-induced hematologic toxicity without adverse impact on tumor response (47). As indicated in pre-clinical studies, properly delayed uridine rescue results in a faster clearance of 5-FU from RNA of bone marrow and enhancement of the rate of recovery of DNA synthesis (39).

Nucleoside transporters are expressed in a variety of cells and tissues with different substrate specificity and selectivity. Most cell types co-express concentrative nucleoside transporters (CNTs) and equilibrative nucleoside transporters (ENTs) to maintain their nucleoside supply. Uridine is mainly accumulated in cells of different origin by the Na^+-dependent CNT1 (SLC28A1) but also by CNT3 (SLC28A3) that has broader substrate specificity. ENTs, particularly ENT1 (SLC29A1) and ENT2 (SLC29A2), mediate facilitated diffusion transport with broader selectivity but relatively low affinity. Recent studies have indicated

that ENT1 is a sort of housekeeping transporter and its expression is often high and is highly retained in tumors. (48).

A clinical study using a tissue array on 300 paraffin-embedded gynecological tumors (endometrium, ovary, and cervix) showed that hENT1 and hENT2 protein expression were highly retained, but a significant number of tumors were hCNT1 negative (49). A more recent breast cancer study has shown that the percentage of hCNT1-positive cells correlates positively with a reduced long-term survival in patients treated with cyclophosphamide/methotrexate/5-fluorouracil (CMF) chemotherapy (50). It is reasonable to speculate that high expression of hCNT1 could be linked to high nucleotide salvage efficiency interfering with 5-FU nucleoside metabolism and ultimately with its anti-proliferative activity.

In summary, this study determined the metabolism and tissue distribution of 5-FU in *UPase* −/− mice and proved the role of UPase in the activation and antitumor activity of 5-FU and Capecitabine. This study also demonstrated the pathological basis for host protection by UPase abrogation from 5-FU and Capecitabine lesions, the ability of uridine to protect the normal tissues and exhibited the effect of tumor-specific expression of *UPase* on the therapeutic efficacy of these agents.

Acknowledgments

This work was supported in part by grants from the National Cancer Institute CA67035 and CA102121 (GP), the Charlotte Geyer Foundation (GP) and the United States Army Medical Research Breast Cancer Research Program DAMD17-00-1-0508 (DC).

Abbreviation List

ATP	Adenosine-5′-triphosphate
BAU	Benzylacyclouridine
5′dFUR	5′-deoxy-5-Fluorouridine
CNTs	Concentrative nucleoside transporters
DPD	Dihydropyrimidine dehydrogenase
TE	Echo time
ES	Embryonic stem cells
ENTs	Equilibrative nucleoside transporters
FOV	Field of view
^{19}F-MRS	Fluorine-Magnetic Resonance Spectroscopy
5-FU	5-Fluorouracil
FUrd	5-Fluorouridine
FUMP	5-Fluorouridine-5′-monophosphate
FdUMP	5-Fluoro-2′-deoxyuridine-5′-monophosphate
FUTP	5-Fluorouridine-5′-triphosphate
FdUTP	5-Fluoro-2′-deoxyuridine-5′-triphosphate
FUXP	5-Fluoro-ribonucleotide
FID	Free induction decay

IC_{50}	Half maximal inhibitory concentration
HPLC	High-performance liquid chromatography
HPMC	Hydroxypropylmethylcellulose
IL-1α	Interleukin-1α
IFN-γ	Interferon-γ
MTD	Maximum tolerated dose
NADPH	Nicotinamide adenine dinucleotide phosphate
OPRTase	Orotate phosphoribosyl transferase
PRPP	5-Phosphoribosyl-1-pyrophosphate
PRESS	^{1}H Point-resolved spectroscopy sequence
TR	Repeat time
TCA	Trichloroacetic acid
TS	Thymidylate synthase
TLC	Thin layer chromatography
TNF-α	Tumor necrosis factor-α
UMP	Uridine monophosphate
UPase	Uridine phosphorylase
UPase−/−	UPase knockout
WT	Wild-type

References

1. Kanzaki A, Takebayashi Y, Bando H, Eliason JF, Watanabe S, Miyashita H, et al. Expression of uridine and thymidine phosphorylase genes in human breast carcinoma. Int J Cancer. 2002; 97:631–5. [PubMed: 11807789]
2. Liu M, Cao D, Russell R, Handschumacher RE, Pizzorno G. Expression, characterization, and detection of human uridine phosphorylase and identification of variant uridine phosphorolytic activity in selected human tumors. Cancer Res. 1998; 58:5418–24. [PubMed: 9850074]
3. Zhang D, Cao D, Russell R, Pizzorno G. p53-dependent suppression of uridine phosphorylase gene expression through direct promoter interaction. Cancer Res. 2001; 61:6899–905. [PubMed: 11559567]
4. Schwartz EL, Hoffman M, O'Connor CJ, Wadler S. Stimulation of 5-fluorouracil metabolic activation by interferon-alpha in human colon carcinoma cells. Biochem Biophys Res Commun. 1992; 182:1232–9. [PubMed: 1540167]
5. Eda H, Fujimoto K, Watanabe S, Ishikawa T, Ohiwa T, Tatsuno K, et al. Cytokines induce uridine phosphorylase in mouse colon 26 carcinoma cells and make the cells more susceptible to 5′-deoxy-5-fluorouridine. Jpn J Cancer Res. 1993; 84:341–7. [PubMed: 8486533]
6. Cao D, Leffert JJ, McCabe J, Kim B, Pizzorno G. Abnormalities in uridine homeostatic regulation and pyrimidine nucleotide metabolism as a consequence of the deletion of the uridine phosphorylase gene. J Biol Chem. 2005; 280:21169–75. [PubMed: 15772079]
7. Cao D, Pizzorno G. Uridine phosophorylase: an important enzyme in pyrimidine metabolism and fluoropyrimidine activation. Drugs Today (Barc). 2004; 40:431–43. [PubMed: 15319798]
8. Longley DB, Harkin DP, Johnston PG. 5-fluorouracil: mechanisms of action and clinical strategies. Nat Rev Cancer. 2003; 3:330–8. [PubMed: 12724731]

9. Cao D, Russell RL, Zhang D, Leffert JJ, Pizzorno G. Uridine phosphorylase (−/−) murine embryonic stem cells clarify the key role of this enzyme in the regulation of the pyrimidine salvage pathway and in the activation of fluoropyrimidines. Cancer Res. 2002; 62:2313–7. [PubMed: 11956089]
10. Pizzorno G, Cao D, Leffert JJ, Russell RL, Zhang D, Handschumacher RE. Homeostatic control of uridine and the role of uridine phosphorylase: a biological and clinical update. Biochim Biophys Acta. 2002; 1587:133–44. [PubMed: 12084455]
11. Wan L, Cao D, Zeng J, Yan R, Pizzorno G. Modulation of uridine phosphorylase gene expression by tumor necrosis factor-alpha enhances the antiproliferative activity of the Capecitabine intermediate 5′-deoxy-5-fluorouridine in breast cancer cells. Mol Pharmacol. 2006; 69:1389–95. [PubMed: 16397116]
12. Peters GJ, Laurensse E, Leyva A, Lankelma J, Pinedo HM. Sensitivity of human, murine, and rat cells to 5-fluorouracil and 5′-deoxy-5-fluorouridine in relation to drug-metabolizing enzymes. Cancer Res. 1986; 46:20–8. [PubMed: 2415245]
13. Ichikawa W, Uetake H, Shirota Y, Yamada H, Takahashi T, Nihei Z, et al. Both gene expression for orotate phosphoribosyltransferase and its ratio to dihydropyrimidine dehydrogenase influence outcome following fluoropyrimidine-based chemotherapy for metastatic colorectal cancer. Br J Cancer. 2003; 89:1486–92. [PubMed: 14562021]
14. de Bruin M, van Capel T, Van der Born K, Kruyt FA, Fukushima M, Hoekman K, et al. Role of platelet-derived endothelial cell growth factor/thymidine phosphorylase in fluoropyrimidine sensitivity. Br J Cancer. 2003; 88:957–64. [PubMed: 12644837]
15. Evrard A, Ciccolini J, Cuq P, Cano JP. Enzyme-prodrug systems: thymidine phosphorylase/5′-deoxy-5-fluorouridine. Methods Mol Med. 2004; 90:263–78. [PubMed: 14657568]
16. Tabata T, Katoh M, Tokudome S, Nakajima M, Yokoi T. Identification of the cytosolic carboxylesterase catalyzing the 5′-deoxy-5-fluorocytidine formation from Capecitabine in human liver. Drug Metab Dispos. 2004; 32:1103–10. [PubMed: 15269188]
17. Hiehle JF Jr, Levine MS. Gastrointestinal toxicity of 5-FU and 5-FUDR: radiographic findings. Can Assoc Radiol J. 1991; 42:109–12. [PubMed: 1828187]
18. Ohta Y, Tezuka E, Tamura S, Yagi Y. Thymosin alpha 1 exerts protective effect against the 5-FU induced bone marrow toxicity. Int J Immunopharmacol. 1985; 7:761–8. [PubMed: 4044100]
19. Pizzorno G, Davis SJ, Hartigan DJ, Russello O. Enhancement of antineoplastic activity of 5-fluorouracil in mice bearing colon 38 tumor by (6R)-5,10-dideazatetrahydrofolic acid. Biochem Pharmacol. 1994; 47:1981–8. [PubMed: 7516657]
20. Laird PW, Zijderveld A, Linders K, Rudnicki MA, Jaenisch R, Berns A. Simplified mammalian DNA isolation procedure. Nucleic Acids Res. 1991; 19:4293. [PubMed: 1870982]
21. Van der Wilt CL, Pinedo HM, Smid K, Peters GJ. Elevation of thymidylate synthase following 5-fluorouracil treatment is prevented by the addition of leucovorin in murine colon tumors. Cancer Res. 1992; 52:4922–8. [PubMed: 1516048]
22. Lu ZH, Zhang R, Diasio RB. Purification and Characterization of dihydropyrimidine dehydrogenase from human liver. J Biol Chem. 2001; 267:17102–9. [PubMed: 1512248]
23. Adams ER, Leffert JJ, Craig DJ, Spector T, Pizzorno G. In vivo effect of 5- ethynyluracil on 5-fluorouracil metabolism determined by ^{19}F nuclear magnetic resonance spectroscopy. Cancer Res. 1999; 59:122–7. [PubMed: 9892196]
24. Weiterova L, Hofer M, Pospisil M, Znojil V, Vacha J, Vacek A, et al. Influence of the joint treatment with granulocyte colony-stimulating factor and drugs elevating extracellular adenosine on erythropoietic recovery following 5-fluorouracil-induced haematotoxicity in mice. Eur J Haematol. 2000; 65:310–6. [PubMed: 11092461]
25. Maring JG, van Kuilenburg AB, Haasjes J, Piersma H, Groen HJ, Uges DR, et al. Reduced 5-FU clearance in a patient with low DPD activity due to heterozygosity for a mutant allele of the DPYD gene. Br J Cancer. 2002; 86:1028–33. [PubMed: 11953843]
26. Diasio RB, Harris BE. Clinical pharmacology of 5-fluorouracil. Clin Pharmacokinet. 1989; 16:215–37. [PubMed: 2656050]
27. Maring JG, Groen HJ, Wachters FM, Uges DR, de Vries EG. Genetic factors influencing pyrimidine-antagonist chemotherapy. Pharmacogenomics J. 2005; 5:226–43. [PubMed: 16041392]

28. Akazawa S, Kumai R, Yoshida K, Ayusawa D, Shimizu K, Seno T. The cytotoxicity of 5-fluorouracil is due to its incorporation into RNA not its inhibition of thymidylate synthase as evidenced by the use of a mouse cell mutant deficient in thymidylate synthase. Jpn J Cancer Res. 1986; 77:620–4. [PubMed: 2427493]
29. Martin DS, Stolfi RL, Sawyer RC, Spiegelman S, Young CW. High-Dose 5-Fluorouracil with Delayed Uridine “Rescue” in Mice. Cancer Res. 1982; 42:3964–70. [PubMed: 7104997]
30. Van Laar JAM, Van der Wilt CL, Rustum YM, Noordhuis P, Smid K, Pinedo HM, et al. Therapeutic efficacy of fluoropyrimidines depends on the duration of thymidylate synthase inhibition in the murine Colon 26-b carcinoma tumor model. Clin Cancer Res. 1996; 2:1327–33. [PubMed: 9816304]
31. Jones L, Hawkins N, Westwood M, Wright K, Richardson G, Riemsma R. Systematic review of the clinical effectiveness and cost-effectiveness of Capecitabine (Xeloda) for locally advanced and/or metastatic breast cancer. Health Technol Assess. 2004; 8:iii, xiii–xvi, 1–143.
32. McGavin JK, Goa KL. Capecitabine: a review of its use in the treatment of advanced or metastatic colorectal cancer. Drugs. 2001; 61:2309–26. [PubMed: 11772141]
33. Reigner B, Blesch K, Weidekamm E. Clinical pharmacokinetics of Capecitabine. Clin Pharmacokinet. 2001; 40:85–104. [PubMed: 11286326]
34. Nishina T, Hyodo I, Miyaike J, Inaba T, Suzuki S, Shiratori Y. The ratio of thymidine phosphorylase to dihydropyrimidine dehydrogenase in tumour tissues of patients with metastatic gastric cancer is predictive of the clinical response to 5′-deoxy-5-fluorouridine. Eur J Cancer. 2004; 40:1566–71. [PubMed: 15196541]
35. Deneen B, Hamidi H, Denny CT. Functional analysis of the EWS/ETS target gene uridine phosphorylase. Cancer Res. 2003; 63:4268–74. [PubMed: 12874036]
36. Kong X, Fan H, Liu X, Wang R, Liang J, Gupta N, et al. Peroxisome Proliferator-Activated Receptor Coactivator-1 Enhances Antiproliferative Activity of 5′-Deoxy-5-Fluorouridine in Cancer Cells through Induction of Uridine Phosphorylase. Mol Pharmacol. 2009; 76:854–60. [PubMed: 19602572]
37. Brown NS, Bicknell R. Thymidine phosphorylase, 2-deoxy-D-ribose and angiogenesis. Biochem J. 1998; 334 (Pt 1):1–8. [PubMed: 9693094]
38. Focher F, Spadari S. Thymidine phosphorylase: a two-face Janus in anticancer chemotherapy. Curr Cancer Drug Targets. 2001; 1:141–53. [PubMed: 12188887]
39. Martin DS, Stolfi RL, Sawyer RC. Use of oral uridine as a substitute for parenteral uridine rescue of 5-fluorouracil therapy, with and without the uridine phosphorylase inhibitor 5-benzylacyclouridine. Cancer Chemother Pharmacol. 1989; 24:9–14. [PubMed: 2720896]
40. Darnowski JW, Handschumacher RE. Tissue-specific enhancement of uridine utilization and 5-fluorouracil therapy in mice by benzylacyclouridine. Cancer Res. 1985; 45:5364–8. [PubMed: 4053009]
41. Darnowski JW, Handschumacher RE. Tissue uridine pools: evidence in vivo of a concentrative mechanism for uridine uptake. Cancer Res. 1986; 46:3490–4. [PubMed: 3708581]
42. Chu SY, Weng ZY, Chen ZH, Rowe EC, Chu E, Naguib FNM, et al. Synthesis of 5-benzyl and 5-benzyloxybenzyl 2,2′-anhydrouridines and related nucleoside analogs as inhibitors of uridine phosphorylase. Nucleosides & Nucleotides. 1988; 7:91–102.
43. Pizzorno G, Yee L, Burtness BA, Marsh JC, Darnowski JW, Chu MY, et al. Clinical and pharmacological studies of Benzylacyclouridine, a uridine phosphorylase inhibitor. Clin Cancer Res. 1998; 4:1165–75. [PubMed: 9607574]
44. Houghton JA, Houghton PJ, Wooten RS. Mechanism of induction of gastrointestinal toxicity in the mouse by 5-fluorouracil, 5-fluorouridine, and 5-fluoro-2′-deoxyuridine. Cancer Research. 1979; 39:2406–13. [PubMed: 156065]
45. Geoffroy FJ, Allegra CJ, Sinha B, Grem JL. Enhanced cytotoxicity with interleukin-1 alpha and 5-fluorouracil in HCT116 colon cancer cells. Oncology Res. 1994; 6:581–91.
46. Pritchard MD, Watson AJM, Potten CS, Jackman AL, Hickman JA. Inhibition by uridine but not thymidine of p53-dependent intestinal apoptosis initiated by 5-fluorouracil: evidence for the involvement of RNA perturbation. Proc Natl Acad Sci USA. 1997; 94:1795–99. [PubMed: 9050858]

47. Schwartz GK, Christman K, Satlz L, Casper E, Ouan V, Bertino J, et al. A phase I trial of a modified, dose intensive FAMTX regimen (high dose 5-fluorouracil+doxorubicin+high dose methotrexate+leucovorin) with oral uridine rescue. Cancer. 1996; 78:1988–95. [PubMed: 8909321]

48. Pastor-Anglada, M.; Casado, FJ. Nucleoside transport into cells: role of nucleoside transporters SLC28 and SLC29 in cancer chemotherapy. In: Peters, GJ., editor. Deoxynucleoside Analogs in Cancer Therapy. Humana Press Publisher; 2006.

49. Farré X, Guillén-Goméz E, Sánchez L, Hardisson D, Plaza Y, Lloberas J, et al. Expression of the nucleoside derived drug transporters hCNT1, hENT1 and hENT2 in gynecologic tumors. Int J Cancer. 2004; 112:959–66. [PubMed: 15386342]

50. Gloeckner-Hofmann K, Guillén-Gómez E, Schmidtgen C, Porstmann R, Ziegler R, Stoss O, et al. Expression of the high-affinity fluoropyrimidine-preferring nucleoside transporter hCNT1 correlates with decreased disease-free survival in breast cancer. Oncology. 2006; 70:238–44. [PubMed: 16837820]

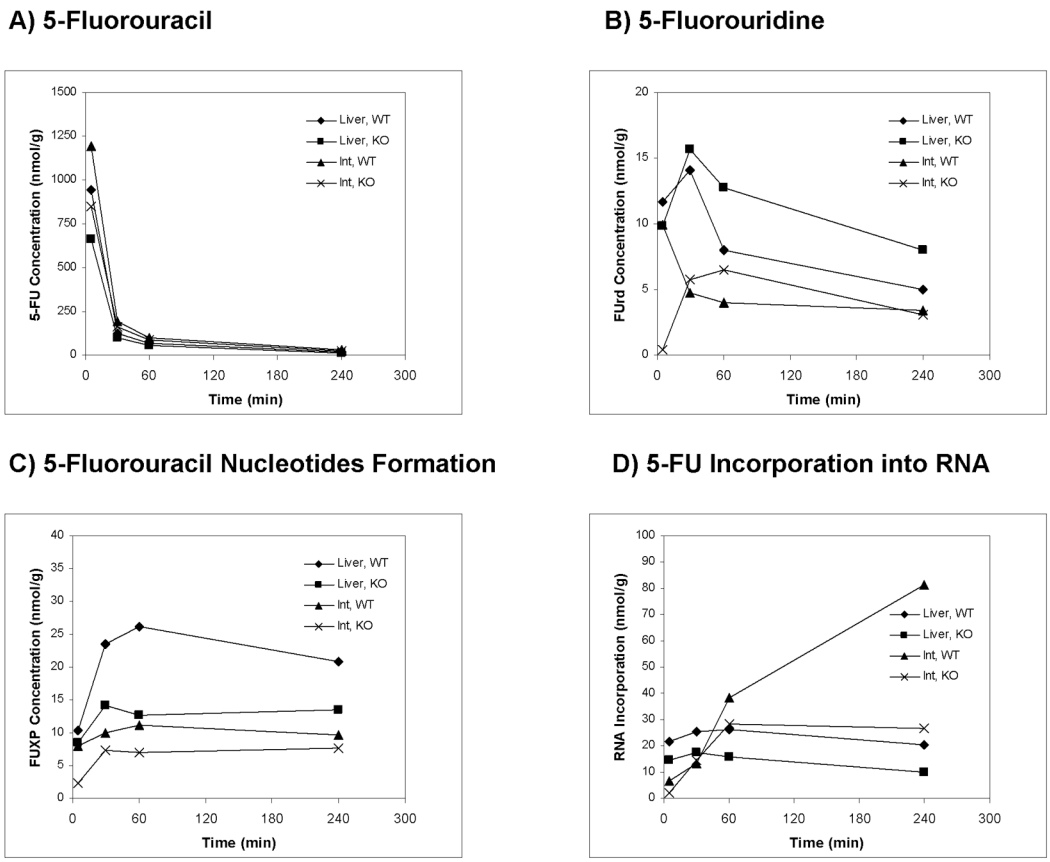

Figure 1. 5-Fluorouracil metabolism and incorporation into liver and intestine RNA

[^{3}H]-5-FU was intravenously administered at 200 mg/kg. The mouse liver and intestinal tissues were collected at 10, 30, 60, and 240 min after injection. Amounts of 5-FU (A), FUrd (B), FUXP (C), and incorporation of 5-FU into RNA (D) were measured as described in Materials and Methods. Values represent results of tissues pooled from three mice. WT, wild-type; KO, uridine phosphorylase knockout; 5-FU, 5-fluorouracil; FUrd, fluorouridine; FUMP, fluorouridine monophosphate; and FUXP, fluorouridine phosphates. Int, Intestine.

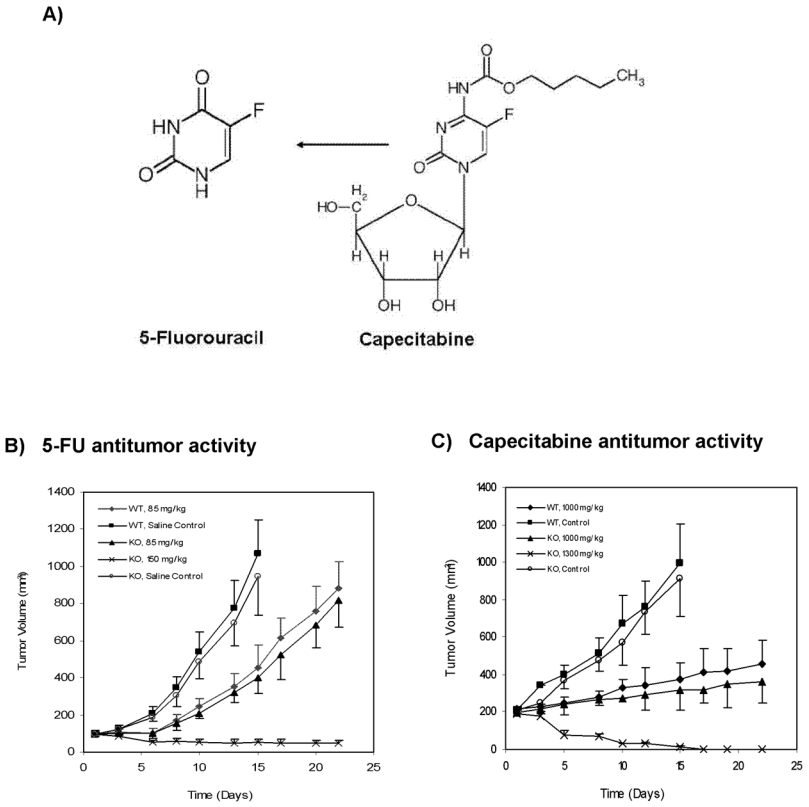

Figure 2. Effect of tumor-specific modulation of UPase on 5-Fluorouracil and Capecitabine antitumor activity

(A) Structural comparison of 5-FU and capecitabine. Colon 38 tumor models were established as described in Materials and Methods. 5-FU (B) was intraperitoneally administered weekly and Capecitabine (C) was delivered orally, 5 days a week, at the indicated doses. Body weight and tumor size were measured every other day. Observations ceased when 20% or more of body weight loss occurred. Presented values represent an average ± SD of 9–11 tumors carried by 6 mice. WT, wild-type; KO, uridine phosphorylase knockout; and 5-FU, 5-Fluorouracil.

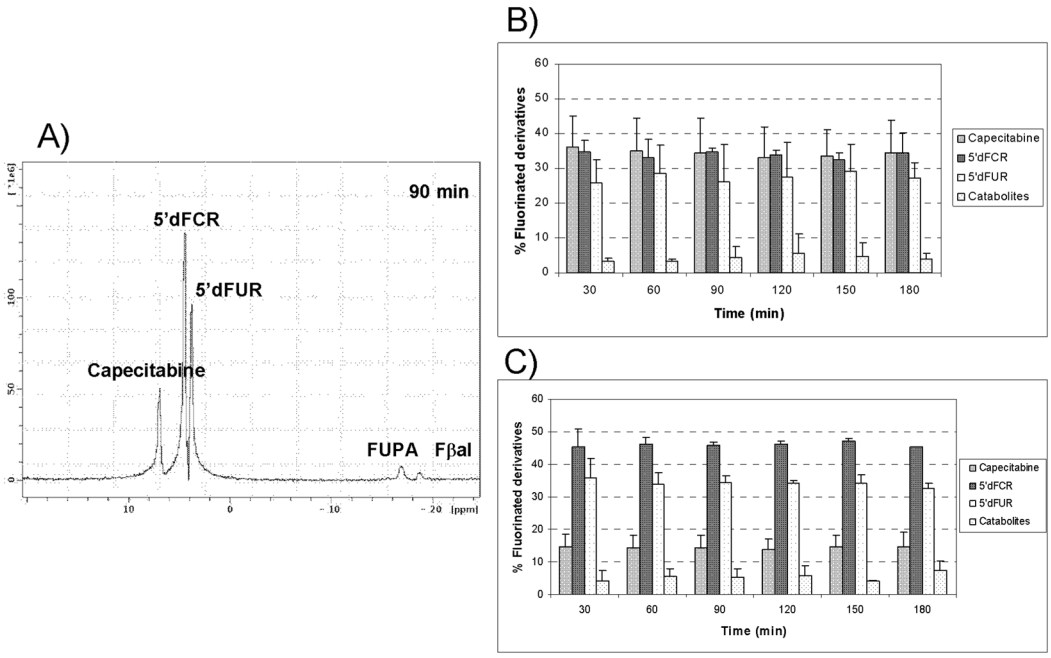

Figure 3. Intratumoral metabolism of Capecitabine by ^{19}F-MRS

Wild-type and UPase −/−mice bearing Colon 38 tumors were treated orally with 1000 mg/kg Capecitabine. Animals were anesthetized with isoflurane and MRS was performed using a Bruker 7T/20 Biospin MRI. A) Presence of fluorinated species in Colon 38 tumors implanted in UPase −/− mice. B) Distribution of Capecitabine metabolites in Colon 38 tumors implanted in wild-type mice. C) Distribution of Capecitabine metabolites in Colon 38 tumors implanted in UPase −/− mice over a 3 hour acquisition time. The values represent the averages of tumor measurements conducted in 6–8 mice per group ± SD.

Table 1

Enzymatic activities in tissues of Wild-Type and UPase −/− mice (nmol/mg/hour)

	UPase		TPase		UK		OPRTase		DPD	
	WT	**UPase −/−**	**WT**	**UPase −/−**	**WT**	**UPase −/−**	**WT**	**UPase −/−**	**WT**	**UPase −/−**
Liver	5.6 ± 1.5	1.3 ± 0.3	25.9 ±6.2	26.7 ±7.3	0.9 ±0.3	1.6 ±0.3*	2.3 ±0.4	2.1 ±0.5	2.0± 0.3	2.0± 0.4
Small Intestine	696.8 ± 80.0	ND	1.9 ± 0.5	2.0 ± 0.5	0.4 ±0.2	0.5 ± 0.2	0.8 ±0.3	0.7 ±0.4	-	-
Colon 38	28.5 ± 4.7	27.9 ± 5.3	0.2 ± 0.1	0.2 ± 0.1	6.6 ±1.5	6.8 ± 1.3	2.5 ±0.2	2.5 ±0.3	-	-

UPase, uridine phosphorylase; TPase, thymidine phosphorylase; UK, uridine kinase; OPRTase, orotate phosphoribosyltransferase; and DPD, dihydropyrimidine dehydrogenase.

+/+, UPase wild type,

−/−, UPase knockout,

ND, not detectable; and

* $p<0.05$ compared to wild type mice.

Table 2

Plasma pharmacokinetic parameters of 5-Fluorouracil and derived 5- Fluorouridine in Wild-Type and UPase −/− mice following a bolus administration of 200 mg/kg of 5-Fluorouracil

Parameter	Units	5-Fluorouracil		5-Fluorouridine	
		WT	UPase −/−	WT	UPase −/−
T_{max}	min	5	5	10	60
C_{max}	μM	3,175.4	2,500.7	3.55	2.71
C_0	μM	5,333.1	5,074.6	-	-
AUC_{inf}	mM-min	85.177	52.385	0.104	-
AUC_{0-240}	mM-min	84.523	52.338	0.105	0.316
$T_{1/2}$	min	37.9	26.3	-	-
CL	mL/min/kg	18.1	29.4	-	-
V_{ss}	mL/kg	633	595.7	-	-

Estimated using WinNonlin V5.2, noncompartmental IV bolus model

Linear up, log down trapezoidal integration rule

AUC_{inf} value is predicted from terminal elimination rate constant

Treated the 0 conc at 240 min for FURD WT as missing

Table 3

Plasma and Tissue concentrations of endogenous Uridine in Wild-Type and UPase −/− mice

	Plasma (μM)		Tissues (pmol/mg)									
		sd	Gut	sd	Kidney	sd	Liver	sd	Spleen	sd	Tumor	sd
WT	1.5	0.6	29.3	3.4	24. 6	3.6	6.4	2.5	4.9	1.1	1.1	0.2
UPase −/−	7.2	2.5	89.3	2.3	71.0	12.6	42.8	7.0	75.2	12.8	7.6	0.7